

# Use of Bandpass Gabor Filters for Enhancing Blood-Myocardium Contrast and Filling-in tags in tagged MR Images

T. Manglik<sup>1</sup>, L. Axel<sup>1</sup>, V. M. Pai<sup>1</sup>, D. Kim<sup>1</sup>, P. Dugal<sup>1</sup>, A. Montillo<sup>2</sup>, Q. Zhen<sup>3</sup>

<sup>1</sup>Radiology, NYU School of Medicine, New York, NY, United States, <sup>2</sup>University of Pennsylvania, Philadelphia, PA, United States, <sup>3</sup>Rutgers University, New Brunswick, NJ, United States

## Introduction

Myocardial tagging provides a quantitative technique for assessing regional myocardial wall motion. Endocardial border detection can be difficult in tagged images due to the presence of tags and low myocardium-to-blood contrast. Also, the tagged MR images pose challenges for both manual and automated segmentation techniques. Gabor filters have been used extensively in image processing techniques [1] and have been recently used for detection of myocardial tags [2]. The purpose of this study was to use 2D Gabor filters to suppress the tags in the myocardium, and enhance the blood-to-myocardium contrast.

## Methods

The Gabor filter acts as a band-pass filter with the central spatial frequency of the filter set equal to the frequency of the tags on the image. The Gabor filter used for

this study was  $h(x,y) = g(x,y) \sin(\omega y + \theta)$ , where  $g(x,y) = \frac{1}{2\pi\sigma_x\sigma_y} \exp(-\frac{(\frac{x}{\sigma_x})^2 + (\frac{y}{\sigma_y})^2}{2})$ ,  $\omega$ : sine wave frequency ( $0.8\omega_{tag} - 1.2\omega_{tag}$ ),  $\omega_{tag}$ : spatial frequency of the

tags,  $\theta$ : sine wave phase ( $0 - 2\pi$ ) and  $\sigma_x$  and  $\sigma_y$  are the standard deviations along x and y, respectively. In this equation, the sine pattern is a function of the distance along y-axis for a horizontal tag pattern. Such a filter will respond to the presence of tags, but not to any other lower or higher spatial frequency component of the image. This technique utilizes the fact that during the MR scan, after the initial tagging, there is a rapid washout of tags within the blood in the cardiac chambers, whereas the myocardial tags fade more slowly over time. The filters used effectively suppressed any low spatial frequency component of the image; this included any untagged blood in the heart. The filters respond to both tag-attenuated and non tag-attenuated regions of the myocardium, thus filling in the tags. Different regions of the tagged myocardium will correspond to different filters in a bank of Gabor filters (consisting of filters with different phase shifts) depending on the amount of initial tag attenuation in that region. Figure 1 illustrates the one-dimensional application of this process. While the first 1D Gabor filter (magenta, 1) responds to minimum-attenuated region of the 1D tag pattern (drawn in black), the other 90° phase shifted Gabor filter (blue, 2) responds to a maximum-attenuated region of the tag pattern. Thus, each of the phase-shifted filters captures a particular amount of attenuation that the initial tagging caused. Figure 2 shows one of the two-dimensional Gabor filters actually used for filtering in image space. While the Fourier domain implementation of the filter banks tends to be much faster to implement and execute, the image domain implementation tends to be easier to understand conceptually.

Figure 3a shows an early-systolic short axis tagged MR image slice that initially had tag lines with frequency  $\omega_{tag}$ . Figures 3b and 3c show how this image (zoomed-in regions-of-interest shown for clarity) responds to Gabor filters from the filter bank with frequency  $\omega_{tag}$  and phase shifts of 0° and 90° respectively. Figure 3d shows a combined result as a maximum of all the images obtained by applying the Gabor filter bank for all  $\omega$  such that  $0.8\omega_{tag} < \omega < 1.2\omega_{tag}$ , (to compensate for change in tag frequency due to motion of the heart wall).

## Results

Manual segmentation of the images by an independent observer was considered to be the gold standard for determining the effectiveness of this technique. The contours outlined by this observer are shown in Figure 3(a). Using these contours on both the original and processed images, we found that the average pixel intensity in the myocardium increased by 22% (due to the “filling-in” of the tags), the average pixel intensity in the blood pool decreased by 47%, and the average blood-myocardium contrast increased by 130%. In order to determine the effectiveness of this technique to assist automated segmentation, we also used active contours to automatically segment the left ventricular (LV) and right ventricular (RV) endocardium of the processed image, and the contours are as shown in Figure 3(d). We computed the number of pixels not common to the manually and automatically drawn contours. The segmentation error was calculated to be the ratio of these pixels to the number of pixels in the endocardial region, and was determined to be 8%.

## Discussion

The Gabor filter bank approach allows us to enhance the blood-to-myocardium contrast, and “fill-in” the tags. The overall smooth structure of the endocardium is maintained. Using a range of values for the tag spacing and phases in the Gabor filters (i.e., the filter bank) allows us to differentiate between the myocardium and blood. The results obtained can be used to augment both manual and automated segmentation processes. A drawback of this technique is that its accuracy depends on the tag-myocardium contrast, and the tag contrast itself decays over time due to T1 relaxation through the cardiac cycle. Also noticeable is the loss in spatial resolution; this loss is dependent on the size of the Gabor filter used. The accuracy of this technique is also limited by tag spacing. Fine structures, such as papillary muscles, that are thinner than the tag spacing may not be detected by the Gabor filters.

## References

[1] J G Daugman, J. Opt. Soc. Am. A, 2(7): 1160-1169, July 1985. [2] Z Qian, et al. IEEE EMBS, Sept 2003. [3] D Dunn, et al. IEEE TPAMI, 16, 130-149, 1994. [4] A. Montillo, et al. MICCAI (1) 2002: 620-633.

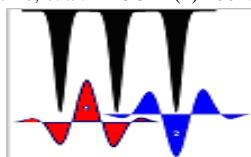


Figure 1 1-D Gabor filter application

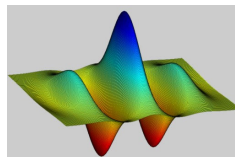


Figure 2. 2-D Gabor Filter

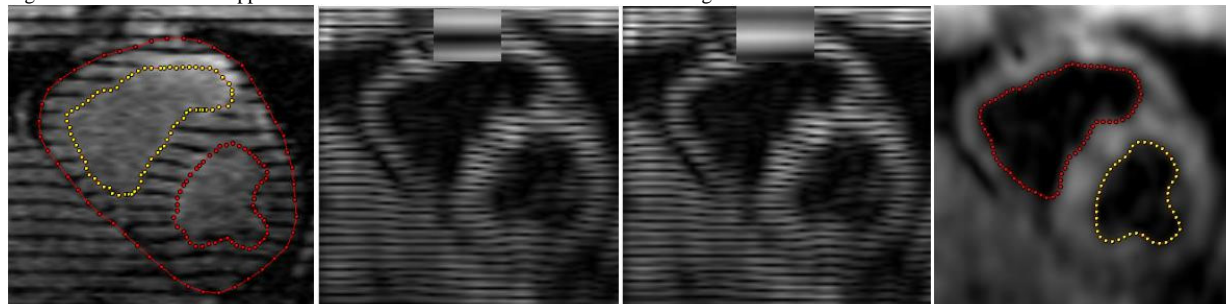


Figure 3(a)

3(b)

3(c)

3(d)